Journal of Neurotrauma

DOI: 10.1089/neu.2022.0419

Transcranial, noninvasive evaluation of the potential misery perfusion during hyperventilation therapy of traumatic brain injury patients

Susanna Tagliabue (susanna.tagliabue@icfo.eu)*

Michał Kacprzak (mkacprzak@ibib.waw.pl)*†

Isabel Serra (isabel.serra@bsc.es)‡

Federica Maruccia (federica.maruccia@icfo.eu)*§

Jonas B. Fischer (jonas.fischer@alumni.icfo.eu)*¶

Marilyn Riveiro-Vilaboa(mriveiro@vhebron.net)/

Anna Rey-Perez (annareyperez@gmail.com)/

Lourdes Expósito (lexposit@vhebron.net)/

Claus Lindner (claus.lindner@me.com)*

Marcelino Báguena (mbaguena@vhebron.net)/

Turgut Durduran (turgut.durduran@icfo.eu)***

María Antonia Poca (pocama@neurotrauma.net)‡ †† ‡‡

Abstract

Hyperventilation (HV) therapy uses vasoconstriction to reduce intracranial pressure (ICP) by reducing cerebral blood volume. However, as HV also lowers cerebral blood flow (CBF), it may provoke misery perfusion (MP) where the decrease in CBF is coupled with increased oxygen extraction fraction (OEF). MP may rapidly lead to the exhaustion of brain energy metabolites, making it vulnerable to ischemia. MP is difficult to detect at the bedside, which is where transcranial hybrid, near-infrared spectroscopies are promising since they noninvasively measure OEF and CBF. We have tested this technology during HV (∼30 minutes) with bilateral, frontal lobe monitoring to assess MP in twenty-seven sessions in eighteen patients with traumatic brain injury. In this study, HV did not lead to MP at a group level ($p>0.05$). However, a statistical approach yielded eighty-nine events with a high probability of MP in nineteen sessions. We have characterized each statistically significant event in detail and their possible relation with clinical and radiological status (decompressive craniectomy and presence of a cerebral lesion), without detecting any statistically significant difference ($p>0.05$). However, MP detection stresses the need for personalized, real-time assessment in future clinical trials with HV, in order to provide an optimal evaluation of the risk-benefit balance of HV. Our study provides pilot data demonstrating that bedside transcranial hybrid near-infrared spectroscopies could be utilized to assess potential MP.

Keywords: Noninvasive, traumatic brain injury, intracranial pressure, intracranial hypertension, hyperventilation treatment, diffuse correlation spectroscopy, time-resolved spectroscopy, misery perfusion

*ICFO - Institut de Ciències Fotòniques, The Barcelona Institute of Science and Technology, Castelldefels, Barcelona, Spain.

†Nalecz Institute of Biocybernetics and Biomedical Engineering, Polish Academy of Sciences (PAS), Warsaw, Poland.

‡Centre de Recerca Matemàtica (CRM), Bellaterra, Spain.

§Neurotraumatology and Neurosurgery Research Unit (UNINN), Vall d'Hebron University Hospital Research Institute (VHIR), Barcelona, Spain.

¶HemoPhotonics S.L., Castelldefels (Barcelona), Spain.

‖Neurotrauma Intensive Care Unit, Vall d'Hebron University Hospital, Barcelona, Spain

**Institució Catalana de Recerca i Estudis Avançats (ICREA), Barcelona, Spain.

††Department of Neurosurgery, Vall d'Hebron University Hospital, Barcelona, Spain.

‡‡Universidad Autònoma de Barcelona, Barcelona, Spain.

Introduction

In severe traumatic brain injury (TBI), intracranial hypertension defined as intracranial pressure (ICP) above 20-22 mmHg predicts neurological deterioration and unfavorable outcome [1–5]. High ICP is a frequent finding in severe TBI [4] and predisposes patients to secondary injuries, especially brain ischemia. Ischemic damage presence in TBI was corroborated in the 1970-80s in *post-mortem* studies [6, 7]. The management of ICP to keep it below a threshold of 20-22 mmHg is a cornerstone goal in managing patients with TBI [8] and is based on the recommendations of the several versions of the Guidelines for the Management of Severe Traumatic Brain Injury endorsed by the Brain Trauma Foundation (BTF), as well as for the Seattle international consensus conference (SIBICC) [5, 9, 10].

For decades, induced hyperventilation (HV) has been a tool to reduce increased ICP [4, 11–13] by provoking a reduction in the partial pressure of arterial carbon dioxide ($PaCO_2$) [14] which triggers vasoconstriction and a consequent decrease in cerebral blood flow (CBF), cerebral blood volume (CBV) and ICP. Despite the widespread use of HV in the different tiers of ICP management, some studies highlighted that indiscriminate use of HV is questionable and may induce global or regional brain ischemia [15, 16], especially important around focal lesions [17].

The heterogeneity in benefits may be due to the reduced CBF in TBI, with undesired consequences which can be understood if we adapt the Siggaard-Andersen classification to the brain [18, 19]. This suggests that when the reduced CBF is uncoupled from the cerebral metabolic rate of oxygen extraction ($CMRO_2$), a simultaneous increase in the oxygen extraction fraction (OEF) occurs, which can lead to ischemic brain hypoxia [18]. The same concept was introduced by Baron et al. [20], who coined the term “misery perfusion” (MP) to describe a hemodynamic profile in which the regional CBF was reduced and the OEF increased [20]. MP is a condition characterized by insufficient blood perfusion to parts of the brain that is unable to deliver the oxygen required to match the oxygen demand [20–23]. For example, in ischemic stroke, MP is considered a predictor of subsequent stroke and its early identification is crucial for its reversal [22].

Going back to the clinical dilemma about the safety of HV, prolonged risk of MP that appears on some individuals may play a strong role in negative outcomes. We hypothesize that the real-time, bedside monitoring of MP risk would be beneficial to develop a personalized HV treatment protocol. As of today, the clinical neuromonitoring tools available at the bedside in the intensive care units (ICU) measure only surrogates of these parameters and often do so invasively (e.g. brain tissue oxygen ($PbtO_2$) monitoring or cerebral microdialysis) or in a discontinuous way (computed tomography, magnetic resonance imaging) [24, 25].

Noninvasive modalities are being tested for neurocritical care monitoring of these populations mainly in research settings. In particular, those based on near-infrared light using diffuse optics (DO) promise a great deal [26, 27].

Continuous wave near-infrared spectroscopy (CW-NIRS) is the only clinically accepted modality and has been widely tested on the TBI population [27, 28], but utility is viewed with skepticism due to the physical limitations that affect its accuracy, precision and its ability to separate extra-cranial signals from intra-cranial ones [27]. The other extreme is time-resolved near-infrared spectroscopy (TRS) [29–31] which contains the highest amount of information per source-detector pair and allows for improved accuracy and precision, albeit with the added complexity of the instrumentation. Both CW-NIRS and TRS are able to measure microvascular blood oxygen saturation and volume.

Another emerging tool is diffuse correlation spectroscopy (DCS), capable of measuring microvascular CBF by using near-infrared light [32–35]. Combining DCS with TRS on the same probe/platform allows for simultaneous estimation of OEF and $CMRO_2$ which we hypothesize will enable us to evaluate the risk of MP. These methods were validated against PET [36, 37] and other techniques. However, CW-NIRS alone was found to be a poor surrogate of CBF, motivating the use of hybrid diffuse optical methods like ours [36]. The aim of this study was to provide a proof-of-principle of noninvasive, comprehensive assessment of MP using hybrid diffuse optics combining TRS and DCS to evaluate their capability for detecting MP due to HV. We sought to characterize MP at a group level and at an individual level TBI patients.

Materials and methods

Clinical population

This is a prospective single-center observational study conducted between June 2016 and October 2020 in patients with TBI admitted to the Neurotraumatology ICU at the Vall d'Hebron University Hospital. The study protocol was reviewed and approved by the clinical research ethics committee of the hospital (ACU-AT-203/2012-3531) and conducted in accordance with the Declaration of Helsinki [38].

Patients who fulfilled the following inclusion criteria were enrolled: 1. patients older than 16 years old with a TBI and a Glasgow coma scale (GCS) score from 3 to 15 at admission who required ICP monitoring and mechanical ventilation from the onset or after clinical deterioration; 2. normocapnia at the time of enrollment defined as an arterial partial pressure of carbon dioxide ($PaCO_2$) between 35-40 mmHg; 3. stable hemodynamic condition at the time of measurement allowing for a short hypocapnic challenge (i.e. absence of lung impairment); 4. preferably but not mandatory, the presence of $PbtO_2$ monitoring; 5. informed consent signed by a legal representative. The study excluded patients with any contraindications for invasive neuromonitoring (concurrent use of anticoagulant drugs, scalp infection, bleeding disorders), clinical signs of brain death, and those whose legal representative did not grant informed consent.

All patients were treated according to 2016 updated version of the BTF clinical guidelines, with the objective of maintaining ICP below 20 mmHg, using stepwise therapy [10]. Patients with refractory intracranial hypertension in the absence of space occupying lesions of a significant volume (> 25 cc) were treated with decompressive craniectomy.

Clinical neuromonitoring

Standard bedside monitors were used to collect physiological parameters and synchronized with the optically-derived ones. ICP was recorded by an intraparenchymal catheter (Camino®, Integra NeuroCare, LifeSciences, USA or Neurovent®-PTO Raumedic® AG multiparameter sensors, DE). $PbtO_2$ was monitored using an

intraparenchymal sensor either by Licox® (Integra NeuroCare, USA) or Neurovent®-PTO (Raumedic®, DE). Information about the sensors placement is reported in the supplementary text 1 (supplementary material).

Mean arterial blood pressure (MABP), oxygen saturation and heart rate were measured by standard probes and recorded by standard monitors (either Solar 8000M/i, GE Healthcare, ES or IntelliVue MX800 or MX750, Koninklijke Philips N.V., NL) monitor. PowerLab hardware (ADInstruments Ltd, UK) and LabChart software (version 6 and 8.1, ADInstruments, NZ) were used to integrate all signals (sampling frequency= 400 Hz), including the synchronization signal from the optical device.

Optical monitors

A custom-built instrument combining TRS and DCS in a similar manner to our previously described systems [39, 40] was utilized. In brief, the TRS module injected light at two wavelengths (690 nm and 830 nm) into the tissue that was detected at a distance of 30 mm on the tissue surface. The DCS module worked at 785 nm and the light was detected at a distance of 25 mm. The two methods acquired data simultaneously at 10 Hz and 40 Hz respectively. Hand-made soft black skin-compatible probes (Eva Rubber, ethylene-vinyl acetate copolymer, 45 Kg/m^3 of density, Materials World, ES) were used to house the source and detection fibers. All modules were controlled and synchronized by the control module and a 10 Hz periodic signal provided the joint time-base for the two optical modules that was recorded externally for synchronization with the other clinical monitors.

Measurement protocol and hyperventilation therapy

The HV protocol consisted of three periods (**Figure 1 B**) with 15 minutes of baseline recording, 30 minutes of HV challenge and 30 minutes of monitoring after restoring the initial baseline respiratory settings. It must be noted that in most cases the duration was adjusted according to clinical care needs and personnel availability. Hypocapnia was induced by changing the ventilator settings (increasing the respiratory rate and/or the

tidal volume) that were modified by the neurointensivist in charge of the patient. Details about the optical probes placement are provided in the supplementary text 1 (supplementary material). One photo prior to putting bandages is shown in **Figure 1 A**.

At baseline, arterial blood samples were taken and analyzed by a co-oximeter (GEM Premier 4000, Werfen, ES) to obtain the initial levels of arterial carbon dioxide ($PaCO_2$) levels. The effectiveness and safety of HV were confirmed by a decrease in $PaCO_2$ of at least 5-6 mmHg in arterial blood samples extracted 10 minutes after the HV challenge was initiated. In case $PaCO_2$ did not confirm a sufficient reduction in $PaCO_2$, additional adjustments to the ventilator settings were conducted. Furthermore, $PaCO_2$ was not allowed to decrease below a 30 mmHg threshold for patient safety considerations.

In each test, the position of the optical probes was recorded by noting the distance between the tip of the TRS detector fiber position and the nasion and the angle between this distance line and the line of the eyes, with zero degrees being on the left side of the face (refer to **Figure 1 C**).

The study protocol allowed for repeated measurements up to three times during the hospitalization. It must be noted that the purpose of this protocol was to evaluate the hemodynamic changes induced by HV and did not have any therapeutic purpose. The neurological outcome of all enrolled patients was evaluated six months after injury by a neuropsychologist by using the Glasgow outcome scale extended (GOSE) [41].

[Figure 1 about here.]

Signal processing of the optical data

All methods are detailed in the supplementary text 2 (supplementary material) and are summarized here.

Optical data were analyzed using standard fitting methods for both TRS and DCS [30, 35, 42]. In this work, we have applied strict data rejection criteria according to the signal-to-noise ratio of the measurement (see the supplementary text 3 in the supplementary material). This resulted in time-traces of oxy- and deoxy-hemoglobin concentrations, blood/tissue oxygen saturation, total hemoglobin concentration and CBF. These were synchronized with the clinical data utilizing common time-base signals.

Further parameters based on both optical and clinical data (i.e. OEF, $CMRO_2$) were derived as well [35, 42]. Then, all data underwent a down sampling to 10 s and further artifact removal. These artifacts were mainly due to clinical procedures which were identified by marks placed electronically in the data during the measurements and, additionally, by the visual inspection of data identifying features such as movement artifacts. Finally, relative values of CBF (rCBF), OEF (rOEF) and $CMRO_2$ ($rCMRO_2$) were calculated as referred to the baseline prior to the beginning of the HV challenge [35].

Statistical methods

Throughout the analysis, the optical data (i.e. a time-trace) from the two cerebral hemispheres were analyzed independently and compared to the data (again a time-trace) representing the systemic (or organ-level) physiology. For example, the changes in CBF were evaluated by the optical measures and hence had two time-traces per patient per measurement session while the ICP time-trace (global brain value) had only one time-trace per patient per measurement session.

Two approaches were utilized. The first approach checked whether the indicators for MP were statistically significant over the whole of HV which is a common approach. The second approach evaluated brief periods of time which takes advantage of the continuous nature of this technology.

For the first approach, the time-traces were divided into baseline period, hyperventilation challenge, recovery, artifacts and transition. Once the artifacts and the transition period (starting at the HV initiation and lasting until HV induction was confirmed by blood gas) were removed, we tested whether the difference between the HV period and the baseline was different from zero by an unpaired Wilcoxon signed-rank test. A type I error of 0.05 was chosen to set significance.

For the second approach, each measurement was evaluated point-by-point for all points in the time series. For details see the supplementary text 4 (supplementary material). In brief, the risk of MP for each point of the time series during HV was evaluated using joint probability indicating a significant CBF reduction concurrent to a significant OEF increase. The resultant time-trace of joint probability was then smoothed in time and a joint-probability threshold of 0.5 was considered to identify time-points

with a significant risk of MP. We note that this threshold is arbitrary and should, in the future, be tuned according to the clinical goals.

Some data was discarded from the MP analysis since either CBF or OEF time-trace was missing, i.e. only those where both were included were used. Initially, a full acquisition was labeled as having the risk of MP if at least one point of the measurement had a probability value higher than 0.5. Then, MP events were recognized separately when there was at least one point above 0.5 (10 s resolution) and their duration lasted until consecutive following points were still above 0.5. All MP events were identified and their duration was quantified. Additionally, a "MP score index" ($MPSC_i$) was calculated for each time-trace for each hemisphere as the ratio between the sum of all time periods during which events of MP were identified (all points above 0.5) and the total time of the HV, excluding transition periods, and was multiplied by 100 to be expressed as a percentage. Presumably, the higher this number, the higher the severity of MP is, but this statement should be quantified with further clinical studies in the future.

MP presence and the clinical status

The possible association of MP occurrence with the clinical condition of the patient was explored. In particular, it was hypothesized that (1) the presence of decompressive craniectomy and (2) the presence of a lesion, both in the measured cerebral hemisphere, were factors that can influence the presence of MP.

Decompressive craniectomy was simply considered to be present or not in the measured cerebral hemisphere.

The presence of a cerebral lesion was evaluated as being present in the considered brain hemisphere coinciding with the noninvasive acquisition side.

In order to test the hypotheses, linear models were built and compared to their respective null models to check for significance. The results for all cerebral measurements in all sessions were considered together as one group, accounting for repeated measurements on the same subject. All of the hypotheses were tested for both measurements with one or more MP occurrences (those with at least one probability point higher than 0.5) and for $MPSC_i$ as a continuous variable.

Linear mixed effects (LME, function *lmer*) models with the subject identifier as the random effect were used as null models for $MPSC_i$, while generalized linear mixed effect (GLME, function *glmer*, binomial family, logistic regression) models with the subject as a random effect were employed as null models for the MP occurrence variable. Models were considered significant when their p-value was lower than 0.05.

All statistical analyses were done in RStudio (R v4.0.1, R Core Team, 2019, RStudio Inc. v1.2.5042, USA, http://www.rstudio.com).

Results

Eighteen subjects were recruited between June 2016 and October 2020 and twenty-nine HV sessions were conducted within ninety-six hours of injury. **Table 1** shows a summary of the clinical and demographic information indicating the number (n) and percentage. The mean age of the group was 35.7±12 years (min: 16, max: 58 years). Thirteen were men and five women. Regarding the type of lesion at the moment of the study, nine patients presented a diffuse brain lesion, eight an evacuated lesion and one patient had a left focal lesion away from the frontal region (left temporo-occipital contusion). At six months of injury, the median GOSE category was 4 (min: 1, max: 8). One patient died (GOSE= 1). **Table 1** shows details of the type of injury according to the Traumatic Data Bank (TCDB) classification [43] and of the functional results of the patients dichotomized into two groups, i.e. favorable versus unfavorable outcome.

Two entire measurements had to be discarded, one due to poor signal quality and one due to the failure of the acquisition software, reducing the useful measurements to twenty-seven. Details about the processes for discarding data are in the supplementary text 3 (supplementary material).

The ICP sensor was absent during one HV challenge (1/27). $PbtO_2$ sensor was absent in six HV sessions (6/27), while it was inserted but not working in two measurement days (2/27). MABP measurements were available in 14/27 sessions corresponding to 7/18 of the subjects. A separate analysis of the effect of MABP on the measurements was, therefore, not warranted.

ICP decreased significantly in twenty-four (24/26) HV sessions in which the sensor was present ($p<0.05$). $PbtO_2$ increased significantly in six (6/19) ($p<0.05$) and decreased significantly in twelve (12/19) measurement days ($p<0.05$).

For all twenty-seven measurements, bilateral optical data acquisition from the forehead was attempted with a potential total of fifty-four time-traces for each parameter. TRS data acquisition was successful in forty-six (46/54) and DCS in forty-five (45/54) attempts. The two methods were successful simultaneously in forty (40/54) cases.

In **Figure 2**, two HV challenges for two different measurement sessions and subjects are shown. The 34-year-old man patient in 'Example 1' had a GCS score of 7 at admission and subdural parieto-occipital hematoma on the left-brain hemisphere, with a subarachnoid hemorrhage, and a cerebral hematoma on the right hemisphere with parietal fractures. In 'Example 2' the patient was a 23-year-old man, with an evacuated left parieto-occipital epidural hematoma. The ICP and $PbtO_2$ probes both showed decreased values *, differing from hemodynamic data obtained through the noninvasive optical probe.

The result of the statistical analysis of the time-traces of the optical data is shown in **Table 2**, where the changes (Δ) in the optical variables are calculated as the percent difference from baseline.

Briefly, these results indicate that CBF showed significant changes in forty-three (43/45) time-traces, where twenty of these (20/43) showed a significant decrease ($p<0.05$). Among these, thirteen (13/20) also had a significant increase in rOEF during HV ($p<0.05$). Finally, out of these thirteen, $rCMRO_2$ was found to be either significantly raised or did not show a significant change in two cases (2/13), highlighted by bold font in **Table 2**. Taken all together, this indicates that, using this more traditional approach, MP was observed in fifteen measurement sessions in eleven subjects.

---

* ICP values are known to be negative in cases that have undergone decompressive craniectomy or are measurement with a high angle of the patient backrest [44, 45].

As described above, the second approach assessed the data point-by-point over time. **Figure 3** shows three time-traces comparing OEF and CBF. The red-shaded periods were identified as at high risk of MP.

Table 3 summarizes these results. Overall, at least one period of MP was identified in twenty-two valid time-traces (22/40), with a total of eighty-nine distinct events. Out of these twenty-two time-traces, five had continuous MP, meaning that the risk of MP had a probability greater than 0.5 for the entire HV duration, while the other seventeen showed one or more separate events. The five measurements with continuous MP had an MPSC score of 100%.

Regarding the association of clinical status with MP, a further consideration had to be taken into account. For the measurements where MP was not detected even in one point, the MPSC was scored as 0. This resulted in a zero-inflated group, that is a group in which the probability distribution of being 0 is higher than other observed values. Consequently, only the subset of measurements in which MPSC was not 0 was extrapolated for the evaluation of the relation of MP with parameters.

In detail, MP was not associated with the presence of decompressive craniectomy (p=0.99). As for the presence of brain lesions, all patients had small lesions in the left frontal lobe. Consequently, only the right cerebral hemisphere measurements were considered in the models' evaluation. For the data from the measurements on the right hemisphere, the presence of a lesion in that hemisphere was not associated with MP (p=0.2). There was a lesion in the right hemisphere during nineteen measurements, while eight did not. There were ten measurements where MP was observed, five without MP while an assessment of MP was not possible for four. The remaining eight sessions, on a region without a lesion, only two measurements showed an MP. There was no association between the presence of a local lesion and MPSC (p=0.4).

Discussion

In this paper, we have presented the characterization of different physiological variables undergoing changes provoked by HV and a method to identify potential cerebral injury risk. The latter was identified with the probability of satisfying the MP condition,

described in the literature as a decrease in CBF and increase in OEF in brain tissue, and was assessed here in different ways. We have introduced the transformation of DO-derived signals into probability values to have MP as a new tool to monitor the repercussions of HV.

Overall, the results indicated that at the group level, despite a decrease in ICP, the mean values of the noninvasive variables did not indicate MP risk. As expected, the response was quite heterogeneous, validating our motivation to seek a neuro-monitor for individualized assessments. This heterogeneity manifested both as a high inter-subject variability as well as a high intra-subject variability. To evaluate the consequences of this, we have carried out an analysis for each time-trace and variable separately. When evaluated in this fashion, we could identify cases where the brain was at a risk of MP where thirteen time-traces showed a significant decrease of rCBF together with a significant increase in rOEF. However, this assessment considered data averaged during the HV period and did not consider whether there were any significant, transient periods of MP risk which did not translate into a mean MP risk over the whole period.

In the final evaluation, by taking full advantage of the fact that DO measurements provided continuous data at the bedside, we have evaluated whether we could detect and distinguish different periods of MP risk. This led to twenty-two measurement sessions being classified as showing periods of MP. This analysis approach quantified how probable was an MP event to happen and could estimate for how long and when this started/stopped. Overall, these results verified our hypothesis of being able to detect CBF and OEF changes related to HV and we characterized each event.

How do these results and methods fit into the previous literature? The ongoing controversies regarding the use of HV are in part due to the sometimes heterogeneous definitions of brain ischemia and whether it can be diagnosed in the early stages of severe TBI [10]. However, the BTF guidelines and the SIBICC consensus conference continue to recommend HV as a measure to decrease elevated ICP, but they do warn against its employment during the first twenty-four hours after TBI because of the significantly reduced CBF observed in many patients [10]. One of the seminal studies on ischemia and TBI by Graham et al. [6] raised awareness of the high frequency of neuropathologic ischemic damage in patients who died from TBI. In the 1980s, the same

authors corroborated that ischemic brain damage was still highly prevalent in these patients [7]. We suggest above that this method could personalize the treatment to avoid these complications.

One question would be why NIRS or a CBF measurement method is not sufficient. To that end, we note that it is claimed that a reduction in CBF only is not sufficient to diagnose ischemia without associating tissue hypoxia with it [4, 14, 19]. For instance, it was found that HV-induced hypocapnia triggers tissue hypoxia [46]. When this is coupled by an increase the cerebral metabolic activity, as some studies found that hypocapnia may cause it through different mechanisms [14], leading to a higher cerebral metabolic rate of oxygen ($CMRO_2$) [16], the physiological interpretation becomes very complex. Interestingly, one study has reported that $CMRO_2$ did not change significantly during moderate hyperventilation of $\sim$40 minutes [47]. However, it appears clear that the increase in OEF is essential to define ischemia and to differentiate it from reduced CBF that is coupled with a decrease in $CMRO_2$ and therefore does not represent ischemia. Some clinical studies that focused on $PbtO_2$ monitoring during HV, instead, concluded with controversial results, showing very heterogeneous response with cases of $PbtO_2$ increase, decrease and no change [4,10].

Despite all these tools and knowledge, MP risk is generally diagnosed by MRI [48,49] or $^{15}O_2$-PET [50], although there is no extensive literature to claim a widespread method. Some studies established threshold values under which MP represents an actual risk of irreversible damage [51, 52]. It was not possible to directly compare these values with the findings of this study due to the complexity of the comparison of absolute values from different modalities. The qualitative agreement was found when the measurement sessions were considered as a whole group showing no evidence of MP. This is presumably because of the above-mentioned heterogeneity that is often observed.

Some studies about HV using the methods listed above underlined the following heterogeneous results during HV. A group of studies showed a decrease in CBF, a decrease in CBV, an increase in OEF and unchanged $CMRO_2$ [14, 51, 53]. Others have shown reduced CBF, increased OEF, increased $CMRO_2$ with a heterogeneous response,

and an increased presence of ischemic areas [14, 51]. Yet another result showed decreased $SvjO_2$ and decreased $PbtO_2$, which correlated with poor outcomes and mortality [14]. These findings were indirect attempts to rule out MP after HV with different methods. Moreover, with similar methods, the connection between CBF reduction, ischemia and outcome especially after HV was highlighted. For example, some studies showed a correlation between the decrease in CBF and poor outcome [14] while others identified higher poor outcomes, higher mortality and higher presence of oligemic regions with HV treatment [14].

The increase in CMRO2 that was observed in some cases could be explained by local or global neuro-impairment or damage, hence leading the brain, or the measured region, being in a stage characterized by high OEF (>50% threshold with respect to the initial condition) and low cerebrovascular resistance (<10% threshold with respect to the initial condition). This could occur when the vasodilation is maximal, or due the effects of a “stealing mechanism” that redirects blood flow from the compromised areas to uncompromised ones [54]. Another potential scenario is that HV causes a rapid reperfusion to regions suffering from ischemia which could cause the over-excitation of cellular metabolism or the excessive firing of the neurons [55]. In summary, these and other events may impair the metabolic reserve with areas with low CBF that can become ischemic even without energy failure during HV. Future studies with baseline CMRO2 estimates with newer optical methods and/or with another modality such as positron emission tomography could reveal further insights about the involved mechanisms.

Over time, it became clear that tissue oxygenation plays an important role in this matter. Due to this, one interesting HV monitoring approach, that can be considered a rudimental precursor of the analysis reported in this paper, was developed on the basis of $SvjO_2$ acquisition, i.e. the so-called “optimized hyperventilation” [4, 56–60]. This approach allowed for early detection of the deleterious effects of HV by the continuous or intermittent sampling of the jugular oxygen saturation and arterial oxygen saturation. The difference between these quantities was used to assess the OEF and HV therapy was administered step-wise with the objective to reduce ICP meanwhile maintaining OEF

within the 24-42% range [56, 57] while avoiding abnormal decreases (luxury perfusion) [59]. Following this approach, HV therapy was maximized to reduce raised ICP when OEF had an unchanged or decreasing tendency. On the contrary, if OEF was increasing with high ICP, other treatments were preferred such as mannitol administration [56]. Such a method was taking into account the effect that HV could provoke on tissue oxygenation, however, it could not directly evaluate CBF changes, which were assumed to be mainly a decrease. This method had some success but was not convincing enough to promote HV to the status of a routinely administered therapy.

In relation to $PbtO_2$, the expected behavior is a decrease [14, 51, 61], although this was confirmed in 12/19 subjects, while 1/19 did not change significantly and 6/19 showed a significant increase. The latter may indicate that the cerebral oxygenation ameliorated in the localized area close to the $PbtO_2$ sensor. rOEF showed a significant increase in the same hemisphere for 4 out of these 6 measurements, while there was no decompressive craniectomy on the same cerebral hemisphere. Therefore, the interpretation remains ambiguous and should be investigated in a larger population.

We also partially confirmed the further hypotheses related relationship between the presence of MP (expressed both as the presence of MP in the cerebral hemisphere and $MPSC_i$) and other clinical conditions (craniectomy and presence of lesions).

The presence of craniotomy did not have a significant effect on determining MP presence, although at the observational level the numbers supported the initial hypothesis: there is a lower risk of MP for cases with craniectomy. According to the expectations, a negative correlation was expected, since craniectomy is practiced in order to treat high intracranial hypertension and improve brain condition. However, it is also true that craniectomy was generally performed on the worse cases (refractory intracranial hypertension), a potential source of bias. Another possibility is that the lack of significance is likely owed to the low number of observations and the models would probably become significant with a larger dataset. For this reason, it should be emphasized that this study was not statistically powered to reliably exclude the effect of craniectomy on MP.

Similarly, there was only prevalence of observations (intended as a prevalence of cases out of the total) of the influence of the presence of a cerebral lesion on MP.

In fact, the effect was not significant after testing. This could be explained by the fact that most of the measurements were carried out in patients with diffuse lesions or evacuated lesions where small or residual brain lesions could be far from the monitored regions. Again, it is also possible that our results are due to the insufficient sample size and that we lack of enough statistical power to reliably rule out whether there is an effect.

Overall, the main limitation in the testing of hypotheses was the small sample size. In fact, the prevalence of observations supported the *a priori* hypotheses, although significance was not found. A larger pool of subjects could eventually lead to significance in demonstrating the validity of the hypotheses.

Another limitation included technical problems and the quality of the optical monitoring.

SNR reasons were the main cause of the non-availability of optical data. The cause of poor SNR was inspected with the CT scans and the illness cause revealing anecdotal evidence that brain regions with diffuse lesions and/or with blood/subcutaneous edema near the probed volume led to poor SNR.

A possible criticism could be related to the reduced coverage of the probe in relation to the evaluation of the wellbeing of the whole cerebral hemisphere. One benefit of our approach is that it is practical – two probes placed on the forehead – and a similar comment can be done for invasive sensors which are placed into burr holes within the skull and they only provide information on a tissue region limited to a few millimeter cubed volumes as compared to the DO probing several centimeter cubed volumes. Furthermore, invasive monitoring comes with associated risks and is often constrained to just one cerebral hemisphere. In the future, with an additional probe engineering, DO can follow the advice given by some works indicating the importance of monitoring the regions close to the focal injury or traumatic penumbra [51, 52]. Moreover, also the hemodynamic and metabolic response to HV is heterogeneous both when evaluated at different positions and at times within a patient and in between patients. In principle, more advanced optical methods with more complex analysis/modeling as well as head-gear with a larger coverage area can be utilized [62, 63]. This comes with complexity, instability and cost. In this particular population, further obstacles arise due to the

presence of other sensors, surgical sutures and other physical obstacles. We believe this work provides evidence to motivate such future developments.

Furthermore, as a future direction, these methods allow for the study of the effects of blood carbon-dioxide levels on the cerebral autoregulation comparing those derived from both invasive and non-invasive sensors. In a similar manner, the effect of the cerebral perfusion pressure changes of our data could be investigated in the future.

Martin et al. [64] suggested the use of different phases to identify the evolution of hemodynamics after the injury, the majority of the measurements (N=20) in our study were during the so-called hyperemic phase. Other seven were during the vasospasm phase. A future study design could focus on increasing this time-range to study the effect of different phases. Similarly, a dichotomization of measurements to distinguish the amount of CBF response between the first 24-36 h and the measurements performed 3-4 days after hospital admission could be addressed, as studied by Marion et al. by microdialysis [65].

Finally, our results call for further evaluation of the method to evaluate the benefits of personalized HV treatments. Despite the limitations, the proposed method answers a first- level need about monitoring HV therapy and could guide it in the future, helping clinicians to conduct HV treatments in a personalized manner. Also, it could be used as a tool during other procedures and as an MP-alert tool.

Conclusions

We have presented a proof-of-principle study showing that non-invasive, hybrid, near-infrared diffuse optical monitoring could be utilized in TBI patients to derive indices that are indicative of the probability of misery perfusion. This was done by evaluating data from a period during hyperventilation therapy where a heterogeneous response was observed as expected. This strengthened our premise that bedside neuro-monitoring could allow for the personalized management of the TBI subjects.

Funding

This research was funded by Fundació CELLEX Barcelona, Fundació Mir-Puig, Ajuntament de Barcelona, Agencia Estatal de Investigación (PHOTOMETABO, PID2019-106481RB-

C31/10.13039/501100011033), the “Severo Ochoa” Programme for Centres of Excellence in R&D (CEX2019-000910-S), the Obra social “la Caixa” Foundation (LlumMedBcn), Generalitat de Catalunya (CERCA, AGAUR-2017-SGR-1380, RIS3CAT-001-P-001682 CECH), FEDER EC, European Commission Horizon 2020 (LUCA No. 688303, VASCOVID No. 101016087, TinyBrains No. 101017113, Bitmap No. 675332), LASERLAB-EUROPE V (EC H2020 No. 871124), KidsBrainIT (ERA-NET NEURON), Lux4Med and and la Fundació La Marató de TV3 (2017,2020).

Acknowledgements

We thank all the personnel of Vall d’Hebron hospital of the intensive care unit, doctors and nurses, who helped us in the recruitment, CT reading and patient management. We thankfully acknowledge Dr. J. Sahuquillo for his help in the design of the project and its implementation during the initiation. Furthermore, we acknowledge the help of the Neurotrauma unit Ph.D. students, Lidia Castro, David Sánchez Ortiz, Lavinia-Madalina Herea, Marta Grau and Ángela Sánchez-Guerrero, for their involvement in the recruitment and the management of the clinical monitors.

Authors contribution

All authors have read and approved the manuscript.

CL, MK and TD designed the study. ST, MK and JBF constructed the optical instrumentation. ST and JBF acquired the optical data. ST, FM, JBF acquired the clinical data. MRV, ARP, MB were responsible for patient recruitment and patient handling. LE helped during the acquisitions. ST analyzed the data and wrote the manuscript. TD and MAP supervised the study, contributed to the discussion, and reviewed and contributed to the manuscript. IS provided guidance for the statistical analysis. ST is the guarantor of this work and, as such, has full access to all the data in the study and takes responsibility for the integrity of the data and the accuracy of the data analysis.

Author disclaimer

Turgut Durduran is an inventor on relevant patents. ICFO has equity ownership in the spin-off company HemoPhotonics S.L. Potential financial conflicts of interest and objectivity of research have been monitored by ICFO's Knowledge & Technology Transfer Department. No financial conflicts of interest were identified. Jonas Fischer was an employee in HemoPhotonics S.L. during the data acquisition. His role was defined by the BitMap project and reviewed by the European Commission. No competing financial interests were present for all the other authors.

References

[1] Juul N, Morris JF, Marshall SB, et al. Intracranial hypertension and cerebral perfusion pressure: influence on neurological deterioration and outcome in severe head injury. J Neurosurg 2000; 92(1):1–6; doi: 10.3171/jns.2000.92.1.0001.

[2] Güiza F, Depreitere B, Piper I, et al. Visualizing the pressure and time burden of intracranial hypertension in adult and paediatric traumatic brain injury. Intensive Care Med 2015; 41(6):1067–1076; doi: 10.1007/s00134-015-3806-1.

[3] Dai H, Jia X, Pahren L, et al. Intracranial pressure monitoring signals after traumatic brain injury: A narrative overview and conceptual data science framework. Front Neurol 2020; 11:959; doi: 10.3389/fneur.2020.00959.

[4] Stocchetti N, Maas IR, Chieregato A, et al. Hyperventilation in head injury: a review. Chest 2005; 127(5):1812–27; doi: 10.1378/chest.127.5.1812.

[5] Hawryluk GWJ, Aguilera S, Buki A, et al. A management algorithm for patients with intracranial pressure monitoring: the Seattle International Severe Traumatic Brain Injury Consensus Conference (SIBICC). Intensive Care Med 2019; 45(12):1783–1794; doi: 10.1007/s00134-019-05805-9.

[6] Graham DI, Adams JH, and Doyle D. Ischaemic brain damage in fatal non-missile head injuries. J Neurol sci 1978; 39(2-3):213–34; doi: 10.1016/0022-510x(78)90124-7.

[7] Adams JH, Graham DI, Scott G, et al. Brain damage in fatal non-missile head injury. J clin pathol 1980; 33(12):1132–45; doi: 10.1136/jcp.33.12.1132.

[8] Farahvar A, Gerber LM, Chiu YL, et al. Increased mortality in patients with severe traumatic brain injury treated without intracranial pressure monitoring. Journal Neurosurg 2012; 117(4):729–34; doi: 10.3171/2012.7.JNS111816.

[9] Bullock R, Chesnut RM, Clifton G, et al. Guidelines for the management of severe head Injury. Eur J Emerg Med. 1996; 3(2):109-27; doi: 10.1097/00063110-199606000-00010.

[10] Carney N, Totten AM, Reilly CO, et al. Guidelines for the management of severe traumatic brain injury, fourth edition. Neurosurgery 2017; 80(1):6-15; doi: 10.1227/NEU.0000000000001432.

[11] Muizelaar JP, Van der Poel HG, Li ZC, et al. Pial arteriolar vessel diameter and CO2 reactivity during prolonged hyperventilation in the rabbit. J neurosurg 1988; 69(6):923–927; doi: 10.3171/jns.1988.69.6.0923.

[12] Ren X, Robbins PA. Ventilatory responses to hypercapnia and hypoxia after 6 h passive hyperventilation in humans. J physiol 1999; 514:885-94; doi: 10.1111/j.1469-7793.1999.885ad.x.

[13] Raichle ME, Plum F. Hyperventilation and cerebral blood flow. Stroke 1972; 3 (5):566–75; doi: 10.1161/01.str.3.5.566.

[14] Godoy DA, Seifi A, Garza D, et al. Hyperventilation therapy for control of posttraumatic intracranial hypertension. Front neurol 2017; 8:250; doi: 10.3389/fneur.2017.00250.

[15] Zhang Z, Guo Q, Wang E. Hyperventilation in neurological patients: from physiology to outcome evidence. Curr op anesthesiol 2019; 32(5):568–573: doi: 10.1097/ACO.0000000000000764.

[16] Curley G, Kavanagh BP, Laffey LG. Hypocapnia and the injured brain: more harm than benefit. Crit Care Med 2010; 38(5):1348–59; doi: 10.1097/CCM.0b013e3181d8cf2b.

[17] McLaughlin MR, Marion DW. Cerebral blood flow and vasoresponsivity within and around cerebral contusions. J Neurosurg 1996; 85(5):871–6; doi: 10.3171/jns.1996.85.5.0871.

[18] Siggaard-Andersen O, Fogh-Andersen N, Gothgen IH, et al. Oxygen status of arterial and mixed venous blood. Crit Care Med 1995; 23(7):1284–93; doi: 10.1097/00003246-199507000-00020.

[19] Siggaard-Andersen O, Ulrich A, Gothgen IH. Classes of tissue hypoxia. Acta Anaesthesiol Scand Suppl 1995; 107:137–42; doi: 10.1111/j.1399-6576.1995.tb04348.x.

[20] Baron JC. Mapping the ischaemic penumbra with PET: implications for acute stroke treatment. Cerebrovasc dis 1999; 9(4):193–201; doi: 10.1159/000015955.

[21] Yamauchi H, Higashi T, Kagawa S, et al. Is misery perfusion still a predictor of stroke in symptomatic major cerebral artery disease? Brain 2018; 135(8):2515–2526; doi: 10.1093/brain/aws131.

[22] Baron JC, Bousser MG, Rey A, et al. Reversal of focal " misery-perfusion syndrome " by extra-intracranial arterial bypass in hemodynamic cerebral ischemia. A case study with 150 positron emission tomography. Stroke 1981; 12:454–9; doi: 10.1161/01.STR.12.4.454.

[23] Powers WJ. Misery perfusion in cerebrovascular disease - is it important? Nature Reviews Neurology 2012; 8:479–480; doi: 10.1038/nrneurol.2012.147.

[24] Byrnes KR, Wilson CM, Brabazon F, et al. FDG-PET imaging in mild traumatic brain injury: a critical review. Front neuroenergetics 2014; 5(13):1–24; doi: 10.3389/fnene.2013.00013.

[25] Wang Z, Mascarenhas C, Jia X. Positron emission tomography after ischemic brain injury: current challenges and future developments. Transl stroke res 2020; 11(4):628-642; doi: 10.1007/s12975-019-00765-0.

[26] Kim MN. Applications of hybrid diffuse optics for clinical management of adults after brain injury. Doctoral dissertation (University of Pennsylvania) 2013.

[27] Roldán M, Kyriacou PA. Near-infrared spectroscopy (NIRS) in traumatic brain injury (TBI). Sensors 2021; 21(5):1586; doi: 10.3390/s21051586.

[28] Mathieu F, Khellaf A, Ku JC, et al. Continuous near-infrared spectroscopy monitoring in adult traumatic brain injury: a systematic review. J Neurosurg Anesthesiol 2020; 32(4):288–299; doi: 10.1097/ANA.0000000000000620.

[29] Patterson MS, Chance B, Wilson BC. Time resolved reflectance and transmittance for the non-invasive measurement of tissue optical properties. Appl Opt 1989; 28(12):2331-36; doi: 10.1364/AO.28.002331.

[30] Torricelli A, Contini D, Pifferi A, et al. Time domain functional NIRS imaging for human brain mapping. NeuroImage 2014; 85: 28–50; doi: 10.1016/j.neuroimage.2013.05.106.

[31] Torricelli A, Pifferi A, Taroni P, et al. In vivo optical characterization of human tissues from 610 to 1010 nm by time-resolved reflectance spectroscopy. Phys Med Biol 2001; 46(8):2227–2237; doi: 10.1088/0031-9155/46/8/313.

[32] Carp SA, Dai GP, Boas DA, et al. Validation of diffuse correlation spectroscopy measurements of rodent cerebral blood flow with simultaneous arterial spin labeling MRI; towards MRI-optical continuous cerebral metabolic monitoring. Biomed opt express 2010; 1(2):553-565; doi: 10.1364/BOE.1.000553.

[33] Boas DA, Sakadžic S, Selb J, et al. Establishing the diffuse correlation spectroscopy signal relationship with blood flow. Neurophotonics 2016; 3(3):031412; doi: 10.1117/1.NPh.3.3.031412.

[34] Culver JP, Durduran D, Furuya D, et al. Diffuse optical tomography of cerebral blood flow, oxygenation, and metabolism in rat during focal ischemia. J Cereb Blood Flow Metab 2003; 23(8): 911–924; doi: 10.1097/01.WCB.0000076703.7123.

[35] Durduran T, Yodh AG. Diffuse correlation spectroscopy for non-invasive, micro-vascular cerebral blood flow measurement. NeuroImage 2014; 85:51–63; doi: 10.1016/j.neuroimage.2013.06.017.

[36] Polinder-Bos HA, Elting JWJ, Aries MJ, et al. Changes in cerebral oxygenation and cerebral blood flow during hemodialysis - a simultaneous near-infrared spectroscopy and positron emission tomography study. J cereb blood flow metab 2020; 40(2):328–340; doi: 10.1177/0271678X18818652.

[37] Giovannella M, Andresen B, Andersen JB, et al. Validation of diffuse correlation spectroscopy against 15O-water PET for regional cerebral blood flow measurement in neonatal piglets. J Cereb Blood Flow Metab 2020; 40(10):2055–2065; doi: 10.1177/0271678X19883751.

[38] World Medical Association (2001). World medical association declaration of Helsinki. Ethical principles for medical research involving human subjects. Bulletin of the World Health Organization; 79 (4), 373-374. World Health Organization; doi: 10.1001/jama.2013.281053.

[39] Lindner C, Mora M, Farzam P, et al. Diffuse optical characterization of the healthy human thyroid tissue and two pathological case studies. PLoS ONE 2016; 11(1): e0147851; doi: 10.1371/journal.pone.0147851.

[40] Giovannella M, Contini D, Pagliazzi M, et al. BabyLux device: a diffuse optical system integrating diffuse correlation spectroscopy and time-resolved near-infrared spectroscopy for the neuromonitoring of the premature newborn brain. Neurophotonics 2019; 6(2): 025007; doi: 10.1117/1.NPh.6.2.025007.

[41] Jennett B, Snoek J, Bond MR, et al. Disability after severe head injury: observations on the use of the Glasgow Outcome Scale. J Neurol Neurosurg Psychiatry 1981; 44(4):285–293; doi: 10.1136/jnnp.44.4.285.

[42] Durduran T, Choe R, Baker WB, et al. Diffuse optics for tissue monitoring and tomography. Rep prog phys 2010; 73(7):076701; doi: 10.1088/0034-4885/73/7/076701.

[43] Marshall LF, Bowers Marshall S, Klauber MR, et al. A new classification of head injury based on computerized tomography. J Neurosurg 1991; 75(issue supplement): S14-S20; doi: 10.3171/sup.1991.75.1s.0s14.

[44] Magnaes B. Body position and cerebrospinal fluid pressure. part 1: clinical studies on the effect of rapid postural changes. J Neurosurg 1976; 44(6):687–97; doi: 10.3171/jns.1976.44.6.0687.

[45] Lilja-Cyron A, Andresen M, Kelsen J, et al. Intracranial pressure before and after cranioplasty: insights into intracranial physiology. J Neurosurg 2019; 18:1-11; doi: 10.3171/2019.7.JNS191077.

[46] Carrera E, Schmidt JM, Fernandez L, et al. Spontaneous hyperventilation and brain tissue hypoxia in patients with severe brain injury. J Neurol Neurosurg Psychiatry 2010; 81(7):793–7; doi: 10.1136/jnnp.2009.174425.

[47] Brandi G, Stocchetti N, Pagnamenta A, et al. Cerebral metabolism is not affected by moderate hyperventilation in patients with traumatic brain injury. Crit Care, 2019; 23(1):45; doi: 10.1186/s13054-018-2304-6.

[48] Xie S, Hui LH, Xiao JX, et al. Detecting misery perfusion in unilateral steno-occlusive disease of the internal carotid artery or middle cerebral artery by MR imaging. AJNR Am J Neuroradiol 2011; 32(8):1504–9; doi: 10.3174/ajnr.A2523.

[49] Gordon AL, Goode S, D' Souza O, et al. Cerebral misery perfusion diagnosed using hypercapnic blood-oxygenation-level-dependent contrast functional magnetic resonance imaging: a case report. J med case rep 2010; 4(54):2–6; doi: 10.1186/1752-1947-4-54.

[50] Kobayashi M, Okazawa H, Tsuchida T, et al. Diagnosis of misery perfusion using noninvasive 15O-gas PET. J nucl med 2006; 47(10):1581–1587.

[51] Coles JP, Fryer TD, Coleman MR, et al. Hyperventilation following head injury: effect on ischemic burden and cerebral oxidative metabolism. Crit care med 2007; 35(2): 568–78; doi: 10.1097/01.CCM.0000254066.37187.88.

[52] Cunningham AS, Salvador R, Coles JP, et al. Physiological thresholds for irreversible tissue damage in contusional regions following traumatic brain injury. Brain 2005; 128:1931–1942; doi: 10.1093/brain/awh536.

[53] Diringer MN, Tideen TO, Yundt K, et al. Regional cerebrovascular and metabolic effects of hyperventilation after severe traumatic brain injury. J neurosurg 2002; 96(1): 103–108; doi: 10.3171/jns.2002.96.1.0103.

[54] Nemoto EM, Yonas H, Kuwabara H, et al. Identification of hemodynamic compromise by cerebrovascular reserve and oxygen extraction fraction in occlusive vascular disease. J Cereb Blood Flow Metab 2004; 24(10):1081–9; doi: 10.1097/01.WCB.0000125887.48838.37.

[55] Matsubara S, Moroi J, Suzuki A, et al. Analysis of cerebral perfusion and metabolism assessed with positron emission tomography before and after carotid artery stenting. J neurosurg 2009; 111(1): 28–36; doi: 10.3171/2008.09.17663.

[56] Cruz J. The first decade of continuous monitoring of jugular bulb oxyhemoglobin saturation: Management strategies and clinical outcome. Criti Care Med 1998; 26(2):344–351; doi: 10.1097/00003246-199802000-00039.

[57] Cruz J, Miner ME, Allen SJ, et al. Continuous monitoring of cerebral oxygenation in acute brain injury: injection of mannitol during hyperventilation. J Neurosurg 1990; 73(5):725–30; doi: 10.3171/jns.1990.73.5.0725.

[58] Cruz J. On-line monitoring of global cerebral hypoxia in acute brain injury. relation- ship to intracranial hypertension. J Neurosurg 1993; 79(2):228–33; doi: 10.3171/jns.1993.79.2.0228.

[59] Cruz J. An additional therapeutic effect of adequate hyperventilation in severe acute brain trauma: normalization of cerebral glucose uptake. J Neurosurg 1995; 82(3):379–85; doi: 10.3171/jns.1995.82.3.0379.

[60] Cruz J. Combined continuous monitoring of systemic and cerebral oxygenation in acute brain injury: preliminary observations. Crit care med 1993; 21(8):1225–32; doi: 10.1097/00003246-199308000-00025.

[61] Schneider GH, Sarrafzadeh AS, Kiening KL, et al. Influence of hyperventilation on brain tissue-PO2, PCO2, and pH in patients with intracranial hypertension. Acta Neurochir Suppl 1998; 71:62-5; doi: 10.1007/978-3-7091-6475-4_20.

[62] Ayaz H, Baker WB, Blaney G, et al. Optical imaging and spectroscopy for the study of the human brain: status report. Neurophotonics 2022, 9(Suppl 2):S24001; doi: 10.1117/1.NPh.9.S2.S24001.

[63] Zhao H, Buckley EM. Optimizing diffuse correlation spectroscopy measurements of cerebral blood flow with a multi-layered analytical model. Biophotonics Congress: Biomedical Optics 2022 (Translational, Microscopy, OCT, OTS, BRAIN), Technical Digest Series (Optica Publishing Group, 2022), paper BW1C.4, 27(4): 287–298, 2022; doi: 10.1364/BRAIN.2022.BW1C.4.

[64] Martin NA, Patwardhan RV, Alexander MJ, et al. Characterization of cerebral hemodynamic phases following severe head trauma: hypoperfusion, hyperemia, and vasospasm. J neurosurg 1997, 87(1):9–19; doi: 10.3171/jns.1997.87.1.0009.

[65] Marion DW, Puccio A, Wisniewski SR, et al. Effect of hyperventilation on extracellular concentrations of glutamate, lactate, pyruvate, and local cerebral blood flow in patients with severe traumatic brain injury. Crit Care Med 2002, 30 (12):2619–2625; doi: 10.1097/00003246-200212000-00001.

[66] Vos PE, van Voskuilen AC, Beems T, et al. Evaluation of the traumatic coma data bank computed tomography classification for severe head injury. J Neurotrauma 2001; 18(7):649–55; doi: 10.1089/089771501750357591 .

[67] Wilson JTL, Pettigrew LEL, Teasdale GM. Structured interviews for the Glasgow outcome scale and extended Glasgow outcome scale: guidelines for their use. J Neurotrauma 1998; 15(8):573–585; doi: 10.1089/neu.1998.15.573.

Table 1: Demographic and clinical data (n=18). SD: standard deviation; TBI: traumatic brain injury; GCS: Glasgow Coma Scale; min: minimum; max: maximum.TCDB: Type of brain lesion according to the Traumatic Coma data bank classification [81] in the com- puted tomography (CT) closest to the study. Diffuse injury type I: no visible intracranial pathology are seen on CT scan; Diffuse injury type II: cisterns are present with midline shift 0-5 mm and/or high or mixed-density lesions ≤25cc: Diffuse injury type III: cisterns compressed or absent with midline shift 0-5 mm and/or high or mixed-density lesions ≤25cc; Diffuse injury type IV: midline shift >5mm without high or mixed-density lesion >25cc; Evacuated mass lesion: any lesion surgically evacuated; Non-evacuated mass lesion: high or mixed-density lesion >25cc not surgically evacuated. GOSE: Outcome at six months according to the Glasgow Outcome Scale Extended [82]. Favorable out- come for the GOSE: categories 5 to 8. Unfavorable outcome for the GOSE: categories 1 to 4. * Epidural hematoma (n=5); Subdural hematoma (n=1); Cerebral contusion with acute subdural hematoma (n=2). ** One subject did not have craniotomy during the first measurement, but had it for the second one.

		n (%)
Sex	Woman	5 (27.8)
	Man	13 (72.2)
Age (years; mean ± SD)	35,7 ± 12 (min: 16; max: 58)	
Causes of TBI	Traffic accident	10 (55.6)
	Pedestrian	1 (5.6)
	Fall from own height	3 (16.6)
	Fall from height > 1 meter	4 (22.2)
GCS score at admission	3 – 8 (severe TBI)	14 (77.8)
	9 – 13 (moderate TBI)	3 (16.6)
	14 – 15 (mild TBI)	1 (5.6)
Type of lesion (TCDB)	Diffuse injury type I	0
	Diffuse injury type II	8 (44.4)
	Diffuse injury type III	0
	Diffuse injury type IV	1 (5.6)
	Evacuated mass lesion*	8 (44.4)
	Non-evacuated mass lesion	1 (5.6)
Outcome (GOSE)	Favorable outcome	7 (38.9)
	Unfavorable outcome	11 (61.1)
Decompressive craniectomy	Right hemisphere	1 (5.6)
	Left hemisphere**	7 (38.9)
	Both hemispheres	2 (11.1)
	None	8 (44.4)

Table 2: Summary of the statistical analysis of the optical data during hyperventilation (HV). Non-significant changes are shown in italics. Regardless of statistical significance (p-value $p<0.05$), the direction of the change is indicated as being positive or negative. Darker lines separating rows divide subjects where the first column shows the different HV sessions or measurement days. Even though the data from the two hemispheres are analyzed independently, for readability, we show results from different hemispheres (Left (L) versus right (R) in separate columns within the same row. Bolded fonts indicate results that correspond to a concurrent decrease in cerebral blood flow (CBF), an in- crease in oxygen extraction fraction (OEF) and raised or unchanged cerebral metabolic rate of oxygen ($CMRO_2$). "NA" indicates that the data was discarded due to quality control whereas "NM" implies that measurement was not taken.

	CBF				OEF					$CMRO_2$			
	Δ % L	p-value L	Δ % R	p- value R	Δ % L	p- value L	Δ % R	p-value R		Δ % L	p-value L	Δ % R	p-value R
1	NA		+7.1	<0.001	-0.3	<0.001	-3.9	<0.001	1	NA		+ 2.5	0.035
2	-13.7	<0.001	NA		-2	<0.001	-3.6	<0.001	2	-15.5	<0.001	NA	
3	NA		+1.8	0.013	+ 0.39	0.185	+1.5	<0.001	3	NA		+3.1	<0.001
4	NA		+2.7	0.001	+ 2.6	0.18	-1	0.002	4	NA		+1.7	0.07
5	+4.2	<0.001	-12.8	<0.001	-5	<0.001	-18	<0.001	5	-1.2	0.013	-26	<0.001
6	+2.3	<0.001	-21	<0.001	NA		+4.8	<0.001	6	NA		-17	<0.001
7	+15	<0.001	-15	<0.001	+7.8	<0.001	+12.7	<0.001	7	+24.3	<0.001	-3.7	<0.001
8	+3.7	<0.001	NA		+5.2	<0.001	+0.23	0.233	8	+9.2	<0.001	NA	
9	-26.3	<0.001	-20	<0.001	+6.8	<0.001	+3	<0.001	9	-21.6	<0.001	-18.3	<0.001
10	+16.7	<0.001	+18.6	<0.001	+0.7	0.28	+2.8	<0.001	10	+19	<0.001	+25	<0.001
11	+21	<0.001	+24.2	<0.001	NA		+2.7	<0.001	11	NA		+27.6	<0.001
12	+1.2	0.03	+9.7	<0.001	NA		+2.7	<0.001	12	NA		+12.7	<0.001
13	-9.4	<0.001	- 3.3	0.078	+1.4	0.25	+1.8	0.002	13	-8.3	<0.001	-1	0.22
14	**-8.3**	**<0.001**	+36.3	<0.001	**+9.6**	**<0.001**	+23	<0.001	14	**+ 0.44**	**0.3**	+68	<0.001
15	-23.3	<0.001	+19.5	<0.001	+11.2	<0.001	+16	<0.001	15	-14.8	<0.001	+38.8	<0.001
16	+10.4	<0.001	+4.3	<0.001	+3.4	<0.001	+4.8	<0.001	16	+14.4	<0.001	+9.3	<0.001
17	-12.7	<0.001	- 0.13	0.38	+ 3.6	0.054	+4.6	0.005	17	-9.8	<0.001	+4.4	0.009
18	-14.1	<0.001	+3.34	<0.001	-5.7	<0.001	-7.8	<0.001	18	-18.8	<0.001	-4.9	<0.001
19	+16	<0.001	**-5.3**	**<0.001**	-4	<0.001	**+6.6**	**<0.001**	19	+11.4	<0.001	**+ 0.97**	**0.2**
20	-14.4	<0.001	NM		+2.7	0.031	NM		20	-12.2	<0.001	NM	
21	NA		-2	0.043	+10.3	<0.001	NA		21	NA		NA	
22	NA		-10.8	<0.001	NA		+1.3	0.014	22	NA		-9.6	<0.001
23	NA		-20.5	<0.001	NA		+2.6	<0.001	23	NA		-18.4	<0.001
24	+30.6	<0.001	-12.5	<0.001	+5.4	<0.001	+6	<0.001	24	+37.7	<0.001	-7.3	<0.001
25	+13.92	<0.001	-19.8	<0.001	+7.8	<0.001	+7	<0.001	25	+22.9	<0.001	-14.1	<0.001
26	+33.1	<0.001	+20.9	<0.001	-3.1	<0.001	+5.8	<0.001	26	+28.8	<0.001	+28.8	<0.001
27	-8.2	<0.001	-10.2	<0.001	NA		+2.25	<0.001	27	NA		-8.2	<0.001

Table 3: Summary of the temporal evaluation of the data indicating the number of distinct misery perfusion (MP) events, their duration and the rounded MP score index (MPSC) %. The rows are numbered in the same way as in **Table 2**. "NA" indicates that measurement was not taken or was discarded for that measurement hemisphere. MPSC % is calculated out of the total actual hyperventilation (HV) duration, which corresponds to the HV period without the transition period. Empty cells in the MP duration correspond to either "NA" measurements or to lack of MP events in the measurement.

	MP events		MP durations [s]		$MPSC_i$ %		Actual HV duration
	left	right	left	right	left	right	[s]
1	NA	0			NA	0	3010
2	5	NA	20, 60, 20, 20, 90		8	NA	2719
3	NA	2		120, 540	NA	21	3037
4	NA	1		60	NA	3	1809
5	0	0			0	0	2820
6	NA	8		7360, 110, 30, 40, 10, 10, 60, 20	NA	96	7921
7	1	1	30	1390	2	100	1390
8	1	NA	10		1	NA	1135
9	3	16	10, 30, 3150	10, 20, 10, 70, 10, 60, 30, 20, 90, 30, 10, 80, 10, 430, 10, 1190	95	62	3367
10	0	0			0	0	565
11	NA	0			NA	0	1938
12	NA	0			NA	0	2053
13	2	0	20, 10		2	0	1342
14	5	0	540, 20, 20, 10, 120		85	0	833
15	1	0	1080		100	0	1080
16	0	0			0	0	1200
17	10	2	50, 10 ,10, 10, 10, 10, 10, 130, 150, 10	50, 60	35	10	1156
18	3	0	10, 10, 10		2	0	1282
19	0	9		280, 20, 140, 110, 10, 10, 20, 20, 10	0	65	948
20	1	NA	240		100	NA	240
21	NA	NA			NA	NA	1352
22	NA	10		80, 30, 20, 30, 10, 10, 20, 180, 140, 660	NA	61	1935
23	NA	3		80, 260, 30	NA	51	727.3
24	0	2		310, 540	0	100	850
25	0	1		1060	0	100	1060
26	0	0			0	0	1210
27	NA	2		690, 110	NA	66	1210

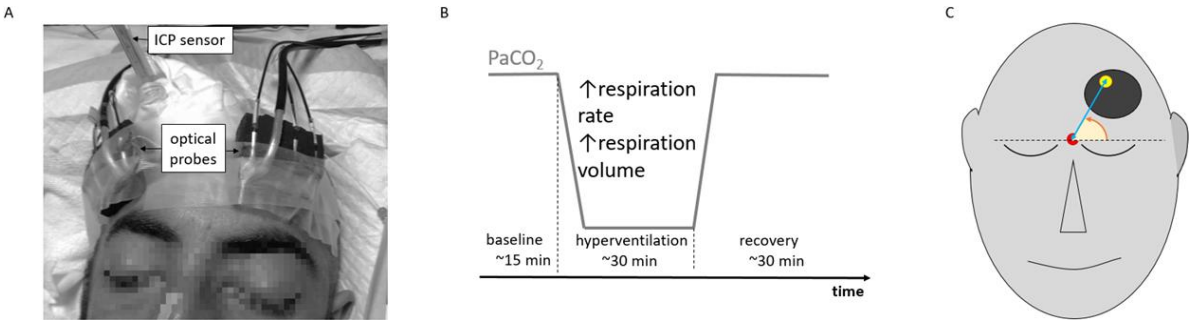

Figure 1: A. A photograph showing the placement of the optical probes where a transparent tape is used to show where the probes are fixed on the skin but in routine clinical measurements, black tapes and bandages are employed. B. Protocol summary showing that, after baseline, HV is induced by increasing the respiratory volume and/or respira- tion rate, then they are brought back to the original values. We note that the protocol duration varied among measurements. C. Drawing of the geometry used to identify the position of the optical probe. The red dot represents the nasion of the patient. The yellow dot shows the TRS source fiber. The double arrow in blue is the radial distance between nasion and the TRS source tip. The orange arrow depicts the angle between this radial distance and the line passing through the nasion, which is perpendicular to the nose line.

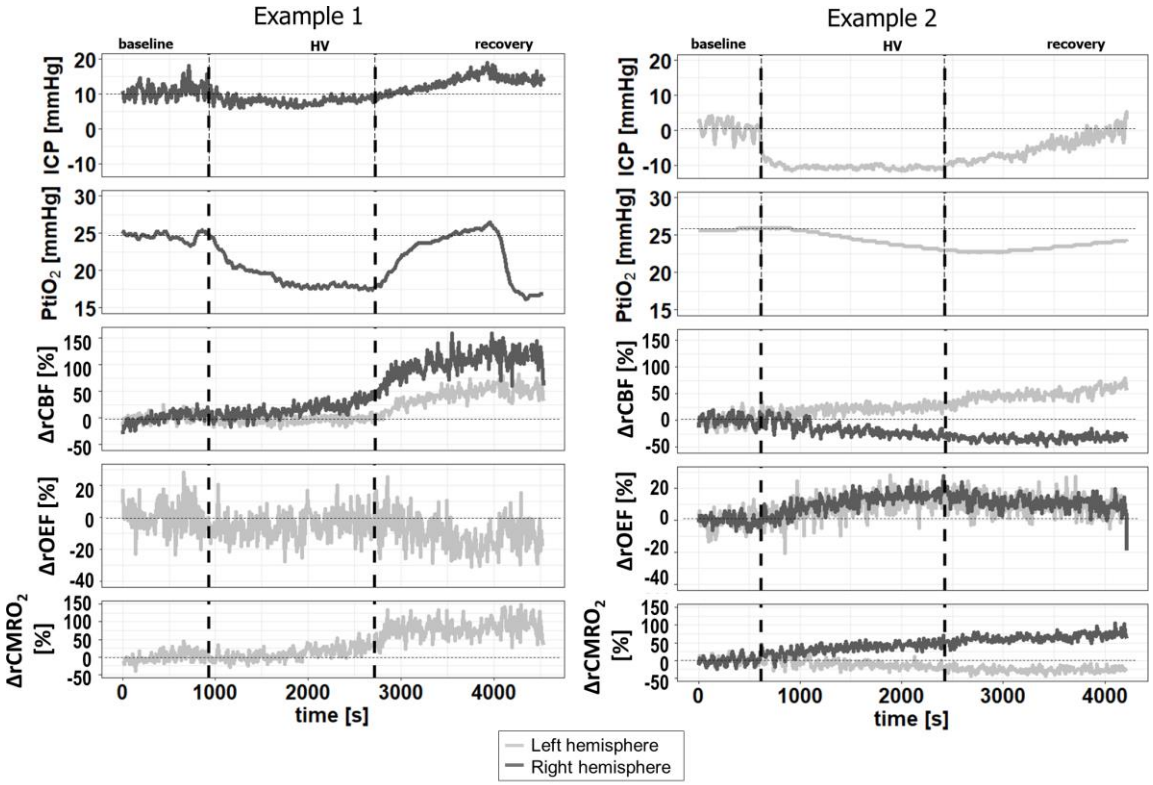

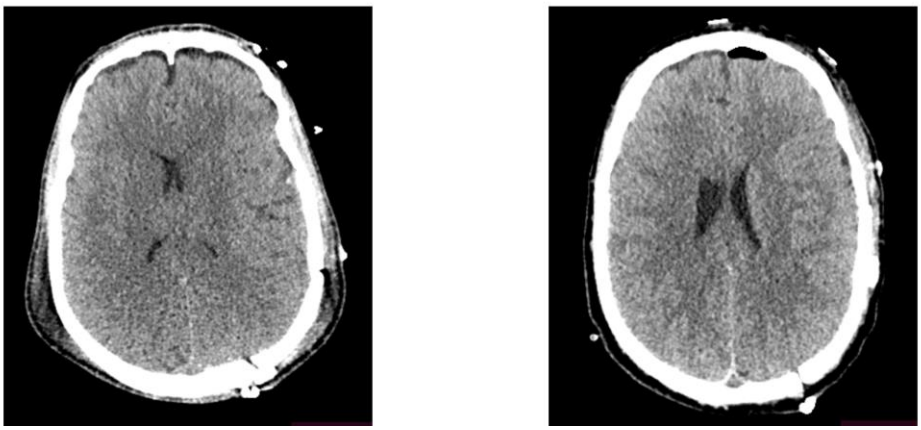

Figure 2: Examples of time-traces of two measurement sessions (columns) from two patients. The 34-year-old male patient in Example 1 had a Glasgow come scale (GCS) of 7 at admission and small or evacuated subdural parieto-occipital hematoma on the left brain hemisphere, with a subarachnoid hemorrhage, while a hematoma and parietal fractures on the right cerebral hemisphere. In Example 2 the patient was a 23-year-old male, with a diffuse injury of type II and GCS=3. Two variables that were collected invasively are shown on the top two graphics while the transcranial, optical measurements are shown below. The vertical dashed lines indicate the period of hyperventilation (HV). Computed tomography (CT) scans of the subjects are also provided.

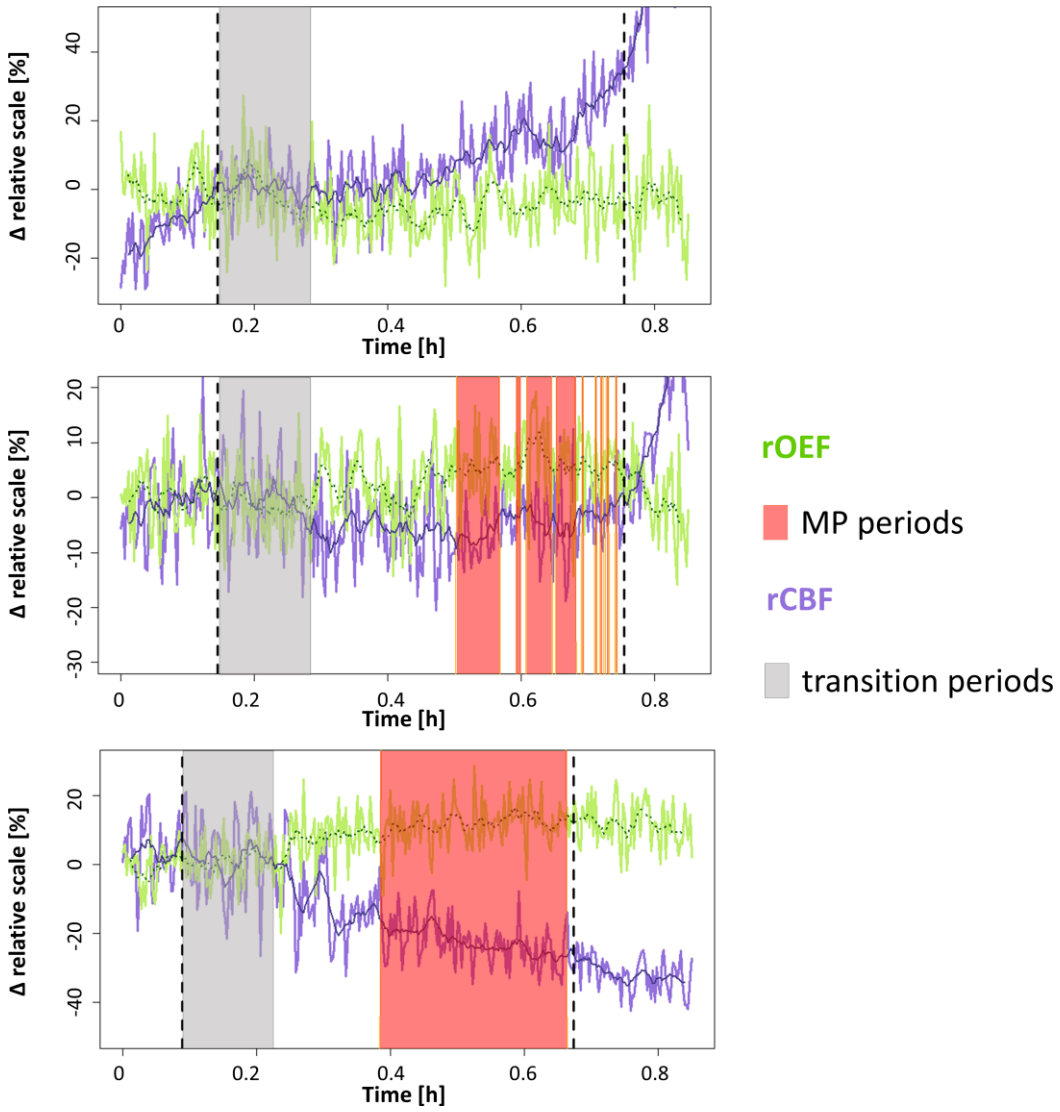

Figure 3: Superposition of misery perfusion (MP) occurrences for timetraces of relative oxygen extraction fraction (rOEF) and relative cerebral blood flow (rCBF) expressed as Δ percent values for three different cerebral hemispheres (in green and purple respectively, with smoothed curves in darker shades of the same colors). Dashed vertical lines define the beginning and the end of the hyperventilation (HV) challenge. MP events are highlighted in red, which define the periods during which the two variables are concomi- tantly moving towards the direction of the MP definition and have a higher probability of risk. The time-traces on the top correspond to the left hemisphere of **Figure 2** Example 1 (on the left of the previous **Figure**), the middle ones correspond to the right hemisphere of the same Example 1, while the bottom time-traces are from the right hemisphere in Example 2 (on the right of **Figure 2**).